RAPID COMMUNICATIONS

PHYSICAL REVIEW B VOLUME 52, NUMBER 12 15 SEPTEMBER 1995-II

Cross-sectional lateral-force microscopy of semiconductor heterostructures and multiple quantum wells

G. Bratina,* L. Vanzetti, and A. Franciosi

Department of Chemical Engineering and Materials Science, University of Minnesota, Minneapolis, Minnesota 55455 and Laboratorio Tecnologie Avanzate Superfici e Catalisi, Istituto Nazionale per la Fisica della Materia, Area di Ricerca, Padriciano 99, I-34012 Trieste, Italy

(Received 23 March 1995)

Lateral-force microscopy and atomic-force microscopy were employed to investigate (110) cross sections of ZnSe-GaAs(001) and $In_{1-x}Ga_xP$/GaAs(001) heterostructures, as well as $Zn_{1-x}Cd_xSe$/ZnSe multiple-quantum-well structures grown by molecular-beam epitaxy. Differences in the dynamic friction coefficient were successfully exploited to image interfaces in air with a lateral resolution better than 3–5 nm for all heterostructures.

The structural and compositional parameters of semiconductor interfaces play a central role in carrier confinement and transport in heterojunctions, and thereby affect the performance of most electronic and optoelectronic devices. Atomic-force microscopy (AFM) is a relatively new but already established experimental probe, which provides morphological information about surfaces with subnanometer resolution,[1] and, in principle, through the analysis of suitable cross sections, can also be applied to interfaces.[2] Measurements of the lateral force acting on the AFM tip during scanning at a constant lateral displacement rate and normal load has been employed to obtain chemical contrast during AFM examinations of composite surfaces.[3] The resulting lateral-force microscopy (LFM) technique has attained atomic resolution in air on selected and relatively inert inorganic materials, including the layer compounds graphite,[3–6] mica,[7,8] and metal dichalcogenides.[6,9]

Here we explore the potential of LFM as a characterization tool of semiconductor heterostructures and multiple quantum wells (MQW's). We focus on material systems highly relevant to present optoelectronics, and present LFM/AFM studies of cleaved (110) cross sections of ZnSe-GaAs(001) and $In_{1-x}Ga_xP$/GaAs(001) heterostructures, as well as $Zn_{1-x}Cd_xSe$/ZnSe(001) MQW's grown by molecular-beam epitaxy (MBE). Recently demonstrated blue-green lasers based on $Zn_{1-x}Cd_xSe$/ZnSe(001) MQW's on ZnSe/GaAs(001) heterostructures,[10,11] as well as the more established infrared lasers based on $In_{1-x}Ga_xP$/GaAs(001) heterostructures,[12] all utilize {110} facets cleaved in air for their Fabry-Pérot cavities.

Most heterostructures were grown by solid-source MBE in a system which includes two interconnected chambers for III-V and II-VI semiconductor fabrication. $In_{0.49}Ga_{0.51}P$/GaAs(001) heterostructures were grown using a gas-source MBE system. All structures were fabricated on GaAs(001) 2×4 buffer layers grown at 580 °C on GaAs(001) wafers.[13] ZnSe epilayers were obtained at 290 °C with a Zn/Se beam pressure ratio near unity, following the procedure described in Ref. 14. $In_{0.49}Ga_{0.51}P$ layers were fabricated at 300 °C, using solid sources for Ga and In, and a PH_3 gas source, as detailed in Ref. 15. $Zn_{1-x}Cd_xSe$/ZnSe MQW's were grown at 250 °C on 1-μm-thick ZnSe buffer layers, with a 30-s growth interruption at each interface. More detail on the growth of the MQW's can be found in Ref. 16. In general, nominal alloy compositions and layer thicknesses were estimated *a priori* from the molecular fluxes employed, and calibrated *a posteriori* using x-ray-diffraction techniques.[13–16] Selected II-VI/III-V heterostructures were protected with Se cap layers deposited at −35 °C, while As cap layers were occasionally used for III-V/III-V heterostructures.

Facets for cross-sectional scanning force microscopy were prepared in air using the three-point loading method illustrated in Fig. 1(a). Prior to cleavage, a notch was fabricated on the (001) surface applying a diamond scriber along one of the ⟨011⟩ directions. An increasing load was then applied along the $[00\bar{1}]$ direction, i.e., from the back of the wafer, to cleave the wafer and expose two {110} facets. Facets 5×7 mm^2 in size were placed on the sample holder of a commercial AFM/LFM instrument, as schematically illustrated in Fig. 1(b). A three-axis, cylindrical piezoelectric crystal manipulator, with a scanning range of 128×128 μm^2 was utilized to change the position of the sample relative to the tip.

We used commercial Si_3N_4 tips with nominal radius of curvature of 40 nm, mounted on triangular stainless steel cantilevers, with 200-μm-long beams and a 50-μm-long base, and a normal elastic constant of 0.12 N/m. The normal load and scanning speed were varied to optimize contrast and overall spatial resolution. Normal loads of about 40 nN and scanning speeds of about 10 μm/s were typically employed. Imaging in the LFM mode and measurements of the lateral force were performed while scanning the tip in the direction perpendicular to the longest axis of the cantilever. Normal forces arising from changes in topography and lateral forces resulting from changes in either friction or topography were detected simultaneously by monitoring the cantilever deflection in the normal and lateral directions, using the displacement of a laser beam reflected off the cantilever and a four-segment photodiode.[17]

In Fig. 2 we show representative AFM (left) and LFM (right) images of a ZnSe-GaAs(001) heterostructure. The results were obtained from the same 4×4 μm^2 region of a (110) cleaved facet, and expose a cross section of the hetero-

 © 1995 The American Physical Society

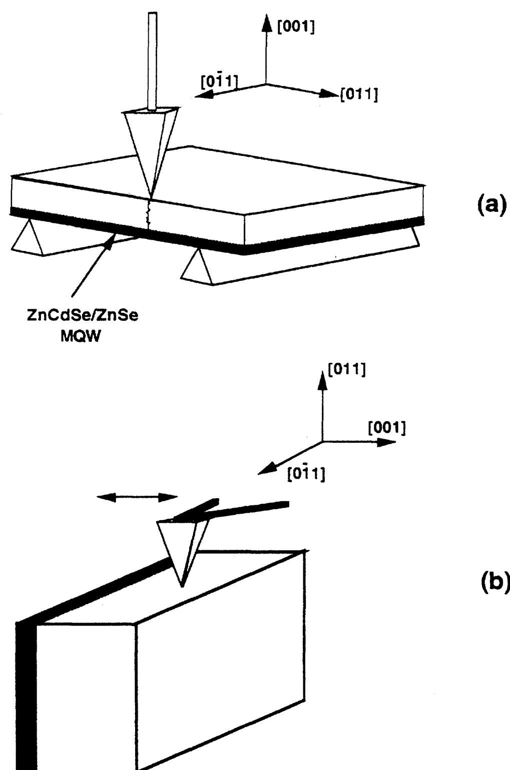

FIG. 1. (a) Schematic representation of the wafer cleavage geometry that yielded minimum areal concentration of cleavage steps in the heterostructure region. The vertical arrow marks the direction of the normal force applied to the wafer during cleavage. (b) Schematic representation of the geometry employed for cross-sectional atomic-force microscopy (AFM) and lateral-force microscopy (LFM) studies.

structure, which consisted of the GaAs buffer, a 1.5-μm-thick ZnSe epilayer, and an amorphous Se cap layer. The heterostructure is fully relaxed[2] (in-plane lattice mismatch between ZnSe and GaAs is 0.27%). Brighter features in the image denote higher elevations of the AFM tip, with the full gray scale corresponding to a height variation of 20 nm.

The facet fabrication procedure illustrated in Fig. 1 exposes μm-size, atomically flat cross sections of the heterostructure, separated by relatively few cleavage-induced defects. Arrows pointing to the left and to the right in Fig. 2 denote two typical cleavage-induced defects. These can be assimilated to 50–100-nm wide trenches 0.32 ± 0.05 nm and 0.92 ± 0.05 nm deep, respectively, the quoted uncertainty corresponding to the standard deviation of the experimental values recorded during repeated measurements of the same features. Such trenches may derive from cleavage steps 1–2 ML high (defining 1 ML as the distance between anions or cations in the direction perpendicular to the cleavage plane or 0.4 nm), arranged in a step-down/step-up sequence.

In the LFM image from the same area (right), regions of apparently higher friction correspond to brighter gray tones.[17] The observed variation in the friction clearly allows identification of the GaAs buffer layer, the 1.5-μm-thick ZnSe epilayer, and the 0.6-μm-thick amorphous Se cap layer. Since we performed sample preparation and analysis in air, humidity and dust particles occasionally give rise in the image to circular defects superimposed to the epitaxial layers. We emphasize that, in the absence of topographical features that influence the lateral deflection of the tip, the contrast in the LFM image of Fig. 2 arises exclusively from nanoscale variations in the dynamic friction coefficient between the tip and the underlying material.

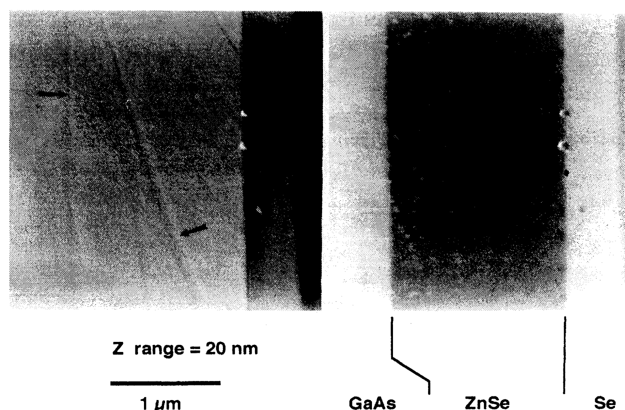

FIG. 2. AFM (left) and LFM (right) images from the same 4×4 μm^2 area of a cleaved (110) facet exposing the interface region of a ZnSe-GaAs(001) heterostructure. The heterostructure is comprised of a GaAs buffer, a 1.5-μm-thick ZnSe epilayer, and an amorphous Se cap layer. Brighter features in the AFM image denote higher elevations of the AFM tip, with the full gray scale corresponding to a height variation of 20 nm. Arrows in the AFM image mark the location of cleavage-induced defects. Darker gray tones in the LFM image denote regions of lower friction.

An example of the overall resolution achievable through cross-sectional LFM for semiconductor heterostructures is illustrated in Fig. 3. In the LFM image, the interface region of a ZnSe-GaAs(001) heterostructure is sampled within a 150×150 nm^2 area, and the chemical contrast deriving from the variation in the dynamic friction coefficient between ZnSe and GaAs allowed us to identify the metallurgical interface with an experimental uncertainty of ±2.0 nm.

In Fig. 4 we show representative AFM (left) and LFM (right) images of $Zn_{0.5}Cd_{0.5}Se/ZnSe(001)$ MQW structures. The results were obtained from the same 290×290 nm^2 region of a (110) cleaved facet, and expose a cross section of

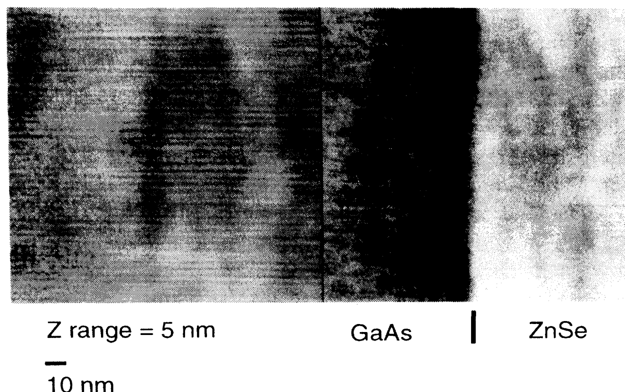

FIG. 3. Detail of the interface region of a ZnSe-GaAs(001) heterostructure probed by cross-sectional LFM within a 150×150 nm^2 area. Darker gray tones in the LFM image denote regions of higher friction (Ref. 17). The chemical contrast deriving from the difference in the dynamic friction coefficient experienced by the tip on ZnSe and GaAs allows identification of the metallurgical interface with an experimental uncertainty of ±2.0 nm.

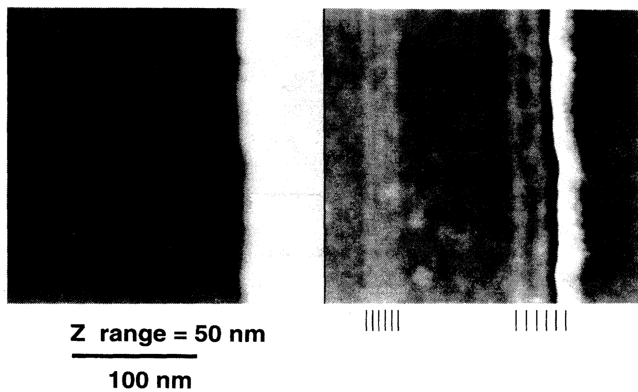

FIG. 4. Cross-sectional AFM (left) and LFM (right) images of $Zn_{0.5}Cd_{0.5}Se/ZnSe(001)$ multiple-quantum-well (MQW) structures. The results were obtained from the same 0.29×0.29 μm^2 region of a (110) cleaved facet, and expose a cross section of two three-period MQW's, with 5- and 10-nm-thick $Zn_{0.5}Cd_{0.5}Se$ wells (see vertical markers on the bottom-most edge of the LFM image) separated by 5- and 10-nm-thick ZnSe barriers, respectively. The two MQW structures are separated by a ZnSe layer with nominal thickness of 100 nm. Brighter features in the AFM image (left) denote higher elevations of the AFM tip, with the full gray scale corresponding to a height variation of 50 nm. Brighter gray tones in the LFM image (right) denote regions of higher lateral deflection of the tip. A 17-nm-high cleavage-induced step is observed by AFM some 60 nm away from the right boundary of the sampled area, and does give rise to appreciable contrast in the LFM image.

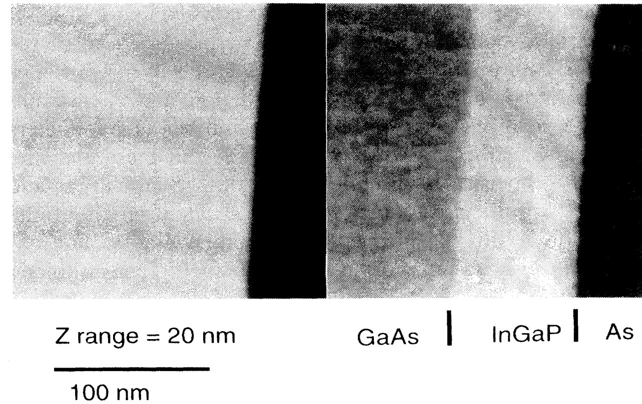

FIG. 5. Cross-sectional AFM (left) and LFM (right) images of a $In_{0.51}Ga_{0.49}P/GaAs(001)$ heterostructure. The results were obtained from the same 200×200 nm^2 region of a (110) cleaved facet, and expose (left to right) portions of the GaAs buffer layer, the 100-nm-thick $In_{0.51}Ga_{0.49}P$ epilayer, and the 0.6-μm-thick amorphous As cap layer. Brighter features in the AFM image (left) denote higher elevations of the AFM tip, with the full gray scale corresponding to a height variation of 20 nm. Brighter gray tones in the LFM image (right) denote regions of lower friction. A 0.30-nm-high cleavage step is observed at the $In_{0.51}Ga_{0.49}P/GaAs$ interface and gives rise to additional contrast in the LFM image.

two three-period MQW's, with 5- and 10-nm-thick $Zn_{0.5}Cd_{0.5}Se$ wells separated by 5- and 10-nm-thick ZnSe barriers, respectively. The two MQW structures are separated by a ZnSe layer with nominal thickness of 100 nm. Brighter features in the AFM image (left) denote higher elevations of the AFM tip, with the full gray scale corresponding to a height variation of 20 nm. Brighter gray tones in the LFM image (right) denote regions of higher lateral deflection of the tip.[17]

The individual quantum wells are clearly detected in the LFM image as vertical parallel bands of higher friction (see vertical markers on the bottom-most edge of the LFM image), that do not correspond to sizable morphological features in the AFM image. Conversely, a 17-nm-high step is observed by AFM some 60 nm away from the right boundary of the sampled area, and extending vertically throughout the image. This major cleavage-induced defect[18] does give rise to appreciable contrast in the LFM image, and appears to be located along the interface between the third well and the topmost ZnSe epilayer.

It is well known that topographical variations may give rise to important LFM contrast due to the mechanical interaction between the tip and the morphological feature during a scan.[5,19,20] In Fig. 4, the up step is encountered during a right-hand scan, and the increased lateral force opposing the motion of the tip results in an enhancement of the signal. The same step scanned in the left-hand direction would correspond to a decrease in the signal. The presence of important morphological features has also a detrimental affect on the lateral resolution of the LFM. For example, when the tip reaches the top of the step the cantilever elastic energy is released through mechanical oscillations, which results in apparent friction variations and contribute to the LFM contrast.

Substantial LFM contrast was achieved also for III-V/III-V heterostructures. In Fig. 5 we show representative AFM (left) and LFM (right) images of a $In_{0.49}Ga_{0.51}P/GaAs(001)$ heterostructure. The results were obtained from the same 200 $\times200$ nm^2 region of a (110) cleaved facet, and expose (right to left) the As cap layer, the 75-nm-thick $In_{0.49}Ga_{0.51}P$ epilayer, and regions of the GaAs(001) buffer. Brighter features in the AFM image (left) denote higher elevations of the AFM tip, with the full gray scale corresponding to a height variation of 20 nm. Brighter gray tones in the LFM image (right) denote regions of lower lateral deflection of the tip.[17]

The $In_{0.49}Ga_{0.51}P$ epilayer is clearly observed in the LFM image as a region of lower friction, with a measured thickness of 75 ± 1 nm, that does not correspond to detectable morphological features in the AFM image. A monoatomic cleavage step propagates at the interface along one $\langle 110\rangle$ direction.

The chemical contrast afforded by the LFM technique for semiconductor heterostructure in air reflects systematic variations in the tip-surface interaction and/or in the mechanical properties of the surface within the semiconductor series. Differences in the friction forces for the different semiconductors were observed for a range of normal loads that spanned the attractive *and* the repulsive regions of the tip-sample interaction potential, although image contrast was generally found to increase with the normal load and was typically greater in the repulsive range.[21] The implication is that more than one microscopic mechanism may contribute to the observed contrast.

It is important to note that sizable contrast is achieved in air notwithstanding that the materials examined are known to develop an oxidized surface layer within minutes upon exposure to atmosphere, and that an adsorbed water/hydrocarbon layer is also expected to rapidly form on all facets in the experimental conditions employed.[5,22] The increase in friction observed in going from ZnSe to

$In_{1-x}Ga_xP$, and to GaAs is difficult to correlate with systematic variations in semiconductor properties in view of the complex nature of the tip-sample interaction in the presence of an unknown amount of surface oxidation, as well as water and hydrocarbon adsorption. Also, a number of parameters required to estimate friction, such as the thickness and mechanical properties of the relevant oxides, the thickness and viscosity of the adsorbed layer, the shear strength of the clean and oxidized surface, etc. are unavailable. For example, at high enough normal load, the coefficient of kinetic friction (μ_{kin}) might be approximated by[23]

$$\mu_{kin} = s/h,$$

where s is the shear strength and h the hardness of the surface, but values of s are hard to come by for clean semiconductor surfaces, let alone oxidized surfaces. Since the shear modulus increase by 40% in going from ZnSe to GaAs (Ref. 24), while the hardness (Mohs scale) increases by a factor of 5.6 (Ref. 25), one could speculate that for clean semiconductors the higher friction should be observed on ZnSe, rather than on GaAs, so that the different experimental behavior might reflect the presence of a thicker and/or more elastic oxide on ZnSe as compared to GaAs. In the absence of comparative systematic oxidation studies of the two surfaces though, one could only point to the higher ionicity and stability of binary Zn-O and Se-O reacted phases as compared to Ga-O and As-O reaction products.

Admittedly, the above argument is only one example of the wide range of speculative arguments that could be proposed based on the available information, and further investigation of the nature of the air-exposed surfaces as well as the detail of the tip-surface interaction is required to conclusively explain the observed systematics.

In conclusion, cross-sectional lateral-force microscopy can be used to image semiconductor heterostructures and quantum wells in air with nanometer resolution. The chemical contrast reflects the substantially higher friction observed during LFM for GaAs relative to ZnSe, for $Zn_{1-x}Cd_xSe$ relative to ZnSe, and for GaAs relative to $In_{1-x}Ga_xP$.

This work was supported in part by the U.S. Army Research Office under Grants Nos. DAAH04-93-G-0206 and DAAH04-93-G-0319, and by the Center for Interfacial Engineering of the University of Minnesota under NSF Grant No. CDR 8721551. We thank M. Nathan and F. Williamson for providing us with $In_{1-x}Ga_xP$/GaAs heterostructures. Discussions with G. Haugstad, E. Kapon, and S. Yang, are gratefully acknowledged.

---

*On leave from Fotona, Stegne 7, 6100 Ljubljana, Slovenia.

[1] G. Binning *et al.*, Phys. Rev. Lett. **56**, 930 (1986).
[2] G. Bratina *et al.*, Proc. SPIE **2346**, 180 (1994).
[3] C. M. Mate *et al.*, Phys. Rev. Lett. **59**, 1942 (1987).
[4] J. Colchero *et al.*, Phys. Status Solidi A **131**, 73 (1992).
[5] D. Baselt and J. D. Baldeschwieler, J. Vac. Sci. Technol. B **10**, 2316 (1992).
[6] H. Heinzelmann *et al.*, Z. Phys. B **88**, 321 (1992).
[7] R. Erlandsson *et al.*, J. Chem. Phys. **89**, 5190 (1988).
[8] S. Fujisawa *et al.*, J. Vac. Sci. Technol. B **12**, 1635 (1994).
[9] C. M. Lieber and Y. Kim, Thin Solid Films **206**, 355 (1991).
[10] See, for example, R. L. Gunshor and A. V. Nurmikko, Proc. SPIE **2346**, 1 (1994).
[11] M. A. Haase *et al.*, Appl. Phys. Lett. **59**, 1272 (1991).
[12] See, for example, S. N. G. Chu and S. Nakahara, Appl. Phys. Lett. **62**, 817 (1993), and references therein.
[13] L. Sorba *et al.*, Phys. Rev. B **46**, 6834 (1992).
[14] R. Nicolini *et al.*, Phys. Rev. Lett. **72**, 294 (1994).
[15] T. J. Miller *et al.*, J. Appl. Phys. **76**, 7931 (1994).
[16] See, for example, R. Cingolani *et al.*, Phys. Rev. B **51**, 15 (1995), and references therein.
[17] Areal mapping of the lateral force in our instrument was performed by detecting the cantilever deflection during the travel of the tip in a selected direction. When the direction is reversed, the electronics reverses the sign of the signal, causing a reversal of the contrast. For images recorded during right-hand scans, areas where higher lateral deflection (higher friction) of the tip was encountered correspond to *brighter* gray tones. For images recorded during left-hand scans, areas where higher lateral deflection (higher friction) of the tip was encountered correspond to *darker* gray tones. For example, ZnSe exhibits a lower friction coefficient both in Figs. 2 and 3, despite the different contrast, in view of the reversed scan direction.
[18] In Ref. 2 we presented several examples of step formation during facet fabrication in strained-layer MQW's involving substantial (2–5 %) lattice mismatch. The steps were found to be located predominantly at the interfaces between $Zn_{1-x}Cd_xSe$ wells and ZnSe barriers, and their height to depend on the lattice mismatch. Possible mechanisms proposed for the occurrence of such steps include crack deviation at the interface between two materials with different fracture toughness, or glide of misfit dislocations.
[19] S. Grafström *et al.*, J. Vac. Sci. Technol. B **12**, 1559 (1994).
[20] G. Haugstad *et al.*, Langmuir **9**, 3717 (1993).
[21] Even when the instrument was operated in the contact mode, in the range of normal loads employed no detectable surface damage was observed as a consequence of the scanning of the tip. This was ascertained by increasing the scan size from 100 nm to 1 μm and checking for tip-induced damage within the smaller area.
[22] N. A. Burnham *et al.*, J. Vac. Sci. Technol. A **9**, 2548 (1991).
[23] T. F. J. Quinn, *Physical Analysis for Tribology* (Cambridge University Press, Cambridge, 1991).
[24] *Group IV Elements and III-V, II-VI, and III-V Compounds*, edited by O. Madelung and M. Schultz, Landolt-Börnstein, New Series, Group III, Vol. 22, Pt. a (Springer-Verlag, Berlin 1987).
[25] *CRC Handbook of Chemistry and Physics*, edited by D. R. Lide (CRC Boston, 1992).

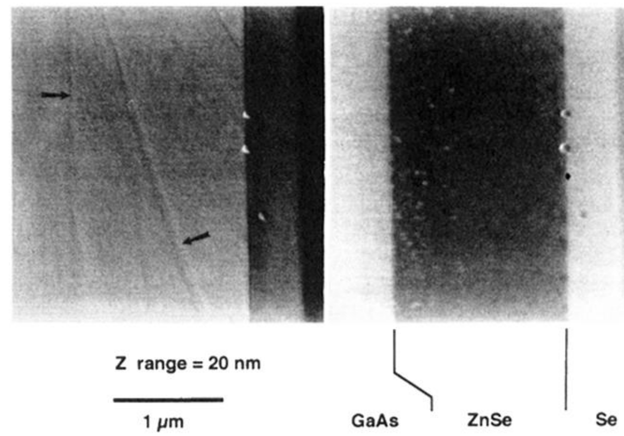

FIG. 2. AFM (left) and LFM (right) images from the same 4×4 μm^2 area of a cleaved (110) facet exposing the interface region of a ZnSe-GaAs(001) heterostructure. The heterostructure is comprised of a GaAs buffer, a 1.5-μm-thick ZnSe epilayer, and an amorphous Se cap layer. Brighter features in the AFM image denote higher elevations of the AFM tip, with the full gray scale corresponding to a height variation of 20 nm. Arrows in the AFM image mark the location of cleavage-induced defects. Darker gray tones in the LFM image denote regions of lower friction.

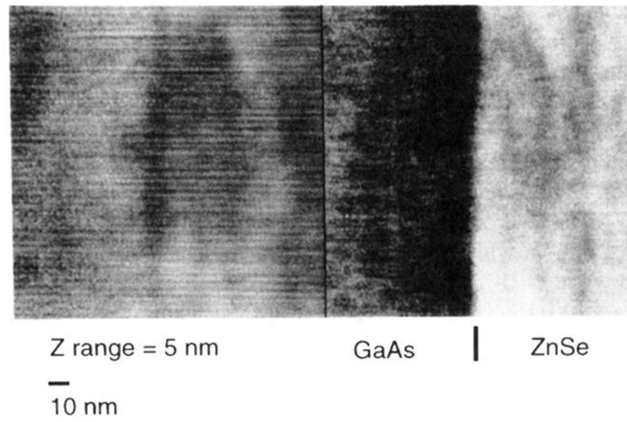

FIG. 3. Detail of the interface region of a ZnSe-GaAs(001) heterostructure probed by cross-sectional LFM within a $150\times150\ \mathrm{nm}^2$ area. Darker gray tones in the LFM image denote regions of higher friction (Ref. 17). The chemical contrast deriving from the difference in the dynamic friction coefficient experienced by the tip on ZnSe and GaAs allows identification of the metallurgical interface with an experimental uncertainty of ±2.0 nm.

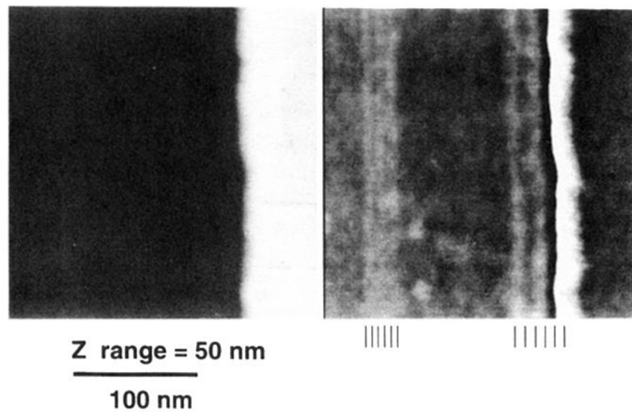

FIG. 4. Cross-sectional AFM (left) and LFM (right) images of $Zn_{0.5}Cd_{0.5}Se/ZnSe(001)$ multiple-quantum-well (MQW) structures. The results were obtained from the same 0.29×0.29 μm^2 region of a (110) cleaved facet, and expose a cross section of two three-period MQW's, with 5- and 10-nm-thick $Zn_{0.5}Cd_{0.5}Se$ wells (see vertical markers on the bottommost edge of the LFM image) separated by 5- and 10-nm-thick ZnSe barriers, respectively. The two MQW structures are separated by a ZnSe layer with nominal thickness of 100 nm. Brighter features in the AFM image (left) denote higher elevations of the AFM tip, with the full gray scale corresponding to a height variation of 50 nm. Brighter gray tones in the LFM image (right) denote regions of higher lateral deflection of the tip. A 17-nm-high cleavage-induced step is observed by AFM some 60 nm away from the right boundary of the sampled area, and does give rise to appreciable contrast in the LFM image.

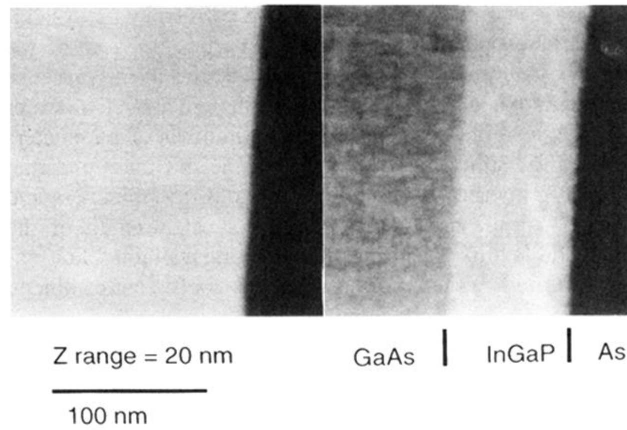

FIG. 5. Cross-sectional AFM (left) and LFM (right) images of a $In_{0.51}Ga_{0.49}P/GaAs(001)$ heterostructure. The results were obtained from the same 200×200 nm^2 region of a (110) cleaved facet, and expose (left to right) portions of the GaAs buffer layer, the 100-nm-thick $In_{0.51}Ga_{0.49}P$ epilayer, and the 0.6-μm-thick amorphous As cap layer. Brighter features in the AFM image (left) denote higher elevations of the AFM tip, with the full gray scale corresponding to a height variation of 20 nm. Brighter gray tones in the LFM image (right) denote regions of lower friction. A 0.30-nm-high cleavage step is observed at the $In_{0.51}Ga_{0.49}P/GaAs$ interface and gives rise to additional contrast in the LFM image.